

**STUDY ON OPTIMIZATION OF TRANSITION IN  
VENTURI FLUME  
FOR VARIOUS WIDTH RATIO**

**A DISSERTATION**

**SUBMITTED IN PARTIAL FULFILLMENT OF THE REQUIREMENTS  
FOR THE AWARD OF THE DEGREE**

**OF**

**MASTER OF TECHNOLOGY  
IN  
HYDRAULICS AND WATER RESOURCES ENGINEERING**

Submitted by

**VARUN KUMAR BARTHWAL**

**(2K21/HFE/05)**

Under the supervision of

**Prof. T.Vijaya Kumar**



**DEPARTMENT OF CIVIL ENGINEERING  
DELHI TECHNOLOGICAL UNIVERSITY**

(Formerly Delhi College of Engineering)

Bawana Road, Delhi-110042

MAY, 2023

**DELHI TECHNOLOGICAL UNIVERSITY**  
(Formerly Delhi College of Engineering)  
Bawana Road, Delhi-110042

**CANDIDATE'S DECLARATION**

I, Varun Kumar Barthwal, (2K21/HFE/05) student of M.TECH (Hydraulics and Water Resource Engineering), hereby declare that the project dissertation titled as **“Study on Optimization of Transition in Venturiflume for various width ratio ”** which is submitted by me to the Department of Civil Engineering, Delhi Technological University, Delhi in partial fulfillment for the award of the degree of Master of Technology, is original and not copied from any source without proper citation. This work has not previously formed the basis for the award of any Degree, Diploma Associateship, Fellowship or other similar title or recognition.

Place: Delhi

(VARUN KUMAR BARTHWAL)

Date:

**DEPARTMENT OF CIVIL ENGINEERING  
DELHI TECHNOLOGICAL UNIVERSITY**  
(Formerly Delhi College of Engineering)  
Bawana Road, Delhi-110042

**CERTIFICATE**

I hereby certify that the Project Dissertation titled as “**Study on Optimization of Transition in Venturiflume for various width ratio**” which is submitted by **Varun Kumar Barthwal, 2K21/HFE/05** Student of **M.TECH (Hydraulics and Water Resources Engineering)**, Department of Civil Engineering, Delhi Technological University, Delhi in partial fulfilment of the requirement for the award of the degree of Master of Technology, is a record of the project work carried out by the student under my supervision. To the best of my knowledge this work has not been submitted in part or full for any Degree or Diploma to this University or elsewhere.

Place: Delhi

**(Prof. T.Vijaya Kumar)**

Date:

**(SUPERVISOR)**

## **ACKNOWLEDGEMENT**

I genuinely convey my profound appreciation and gratitude to Prof. T.Vijaya Kumar for facilitating me with an opportunity to function under their supervision and guidance. Their relentless support, insightful advice and tremendous assistance have motivated me to finish the thesis successfully. I deeply thank them for their critical encouragement and constructive feedback, which helped me to create my own concepts and make my research as exciting as possible.

I am greatly indebted to Mr Vijay Kaushik Research Scholar, Department of Civil Engineering, for their encouragement and guidance, as well as their valuable advice and ideas.

I am thankful for the assistance provided by the Fluid Mechanics and Hydraulics Laboratory of the Civil Engineering Department staff, both with collaborating on the project, and for helping me in any way possible.

The pleasant environment and collaborative business practices at Delhi Technological University made my stay remarkable and pleasurable. The kindness and support of my batchmates and superiors will always remind me of my student days here, and I am immensely grateful. Their advice and guidance were extremely beneficial whenever necessary.

My parents and colleagues provided me with moral courage and assistance throughout the completion of my dissertation, for which I am grateful. Above all, I give thanks to the Lord for bestowing his rewards and love upon me.

Place: Delhi

Date:

(VARUN KUMAR BARTHWAL)

## **ABSTRACT**

A Venturi flume is a device used to calculate the rate of flow of a liquid in considerable amounts. It is based on the Venturi effect, for which it is named. A Venturi flume is a flume with a contracted region situated in its center which, due to the Venturi effect, results in a decrease of fluid pressure at the center of the constriction. By comparing the fluid pressure at the center of the flume with that earlier in the device, the rate of flow can be measured.

In this study, various width ratio of transitions have been made under different discharges for optimising the width at transition to avoid supercritical condition .

From the experiment it has been found for various discharges that the width ratio of 0.36 when the flow becomes critical. In the various width ratio it has been found for width ratio 0.36 the flow at the throat section is just critical and if we further decrease the flow may become critical. For high discharges ,water surface profile increases with the width ratio. But for the low the discharges the water surface for the 0.36 and 0.4 closesly move.

The Froude number is found to be increasing when the discharge is increasing. But it is interesting to see that the width ratio is decreasing but the Froude number at the throat section is going to critical

## **CONTENTS**

	<b>Page No.</b>
<b>Candidate's Declaration</b>	<b>i</b>
<b>Certificate</b>	<b>ii</b>
<b>Acknowledgement</b>	<b>iii</b>
<b>Abstract</b>	<b>iv</b>
<b>Contents</b>	<b>v</b>
<b>List of Figures</b>	<b>vii</b>
<b>List of Tables</b>	<b>ix</b>
<b>CHAPTER 1 INTRODUCTION</b>	<b>1</b>
1.1 Metering Flume	1
1.1.1 Submerged Venturiflume	1
1.1.2 Free Flow Venturiflume	2
1.1.3 Parshall Flume	3
1.1.4 Cutthroat Flume	4
1.2 Necessity of Transition	4
1.3 Definition of Transition	5
1.4 Classification of Transition	6
1.5 General Features of Various Types	9
1.6 Economics of Transition	11
<b>CHAPTER 2 REVIEW OF LITERATURE</b>	<b>13</b>
2.1 Literature Review	
<b>CHAPTER 3 MODELS AND METHODOLOGY</b>	<b>17</b>
3.1 Objective of the Research	17
3.1 Models	18
3.2 Experimental Setup	19
3.3 Tools and Instrumentation	22
3.4 Methodology	26
<b>CHAPTER 4 RESULTS AND DISCUSSIONS</b>	<b>29</b>
4.1 Effect of specific energy for various width ratio	29
4.2 Variation of Froude number with various width ratio	33
4.3 Variation of Froude number and discharge	36

<b>4.4</b>	Plot of water surface profile with different width ratio	<b>37</b>
<b>CHAPTER 5</b>	<b>CONCLUSIONS</b>	<b>40</b>
	<b>Future Scope</b>	<b>41</b>
	<b>References</b>	<b>42</b>

## List of Figures

<b>Figure No.</b>	<b>Title</b>	<b>Page No.</b>
1.1	Submerged Venturiflume	2
1.2	Free flow flu	3
1.3	Cut throat flume	4
1.4	Basic Subcritical flow transition types	8
1.5	Wedge-type Transition from rectangular trapezoidal channel	11
3.1	Model 1 with width ratio (0.5)	19
3.2	Model 2 with width ratio (0.4)	19
3.3	Model 3 with width ratio (0.36)	20
3.4	Experimental Setup	21
3.5	Digital Manometer	22
3.6	Diagram of Electromagnetic Flowmeter	24
3.7	Schematic diagram of electromagnetic flowmeter	25
3.8	Measurement of velocity with the help of pitot tube	27
3.9	Measurement of depth	27
4.1	Specific Energy curve for width ratio (0.5)	29
4.2	Specific Energy curve for width ratio (0.4)	30
4.3	Specific Energy curve for width ratio (0.36)	30
4.4	Specific Energy curve for various width ratio	31
4.5	Variation of Froude number with width ratio at disc. 40/l s	33



### **List of Figures**

<b>Figure No.</b>	<b>Title</b>	<b>Page No.</b>
4.6	Variation of Froude number with width ratio at disc. 35/l/s	34
4.7	Variation of Froude number with width ratio at disc. 30/l/s	34
4.8	Variation of Froude number with width ratio at disc. 25/l/s	35
4.9	Variation of Froude number with width ratio at disc. 20/l/s	35
4.10	Variation of Froude Number and discharge	36
4.11	Water surface profile for width ratio (0.5)	37
4.12	Water surface profile for width ratio (0.4)	37
4.13	Water Surface profile for width ratio (0.36)	38
4.14	Water Surface Profile with different width ratio at Q (40l/s)	38
4.15	Water Surface Profile with different width ratio at Q (30l/s)	39
4.16	Water Surface Profile with different width ratio at fixed Q (20l/s)	39

### **List of Tables**

<b>Table No</b>	<b>Title</b>	<b>Page No.</b>
1	Transition loss coefficient	9
2	Reading for the experiment for width ratio (0.5)	32
3	Reading for the experiment for width ratio (0.4)	32
4	Reading for the experiment for width ratio (0.36)	32

# CHAPTER 1

## INTRODUCTION

### 1.1 Metering Flumes

A metering flume, also known as a flow measurement flume, is a man-made channel segment used to measure canal discharge. Flumes come in a variety of sizes and materials, including aluminium, fibreglass, steel, and wood.

A Venturiflume is a device which is used to measure the flow rate of fluids in open channels. It consists of a converging section, throat, and diverging section, similar to a Venturimeter. The flow rate is calculated by measuring the difference in pressure between the throat and the upstream section of the flume. The design of a Venturi flume involves determining the dimensions of the converging and diverging sections to ensure accurate flow rate measurements. The following classifications of the metering flume are described below

- I. Submerged Venturi Flume
- II. Free flow Venturi Flume
- III. Parshall Flume
- IV. Cut-throat Flume

#### 1.1.1. Submerged Venturiflume

The upstream throat segment of the submerged Venturi flume gradually contracts and the downstream throat section expands. Because the downstream level of the flume is kept equal to the level of the throat section, retrograde flow into the throat section is possible. As a result, it is referred to as a submerged Venturi flume.

Two head measurements are necessary to measure discharge in a submerged Venturi flume, one at the entry and one at the throat. Stilling wells at the entry and neck are used to take these measurements. The volume of water released through the flooded Venturi's discharge can be estimated by using the following formula.

$$Q = \frac{c_d a_1 a_2 \sqrt{2gh}}{\sqrt{a_1^2 - a_2^2}} \quad (1)$$

Where,

$a_1$  = Area at the entrance of the venturi flume

$a_2$  = Area at the throat of the venturi flume

$g$  = acceleration due to gravity

$h$  = head difference between two stilling wells

$C_d$  = Coefficient of discharge of Venturi flume



Fig 1.1 Submerged Venturi flume

### 1.1.2. Free flow Venturi Flume

Free-flow venturi flumes are sometimes known as standing wave flumes because they are designed to create a standing wave on the downstream portion of the flume. To form a hydraulic leap, the level of the downstream portion of the flume is kept lower than the level of the throat. As a result, the discharge through the throat segment is solely determined by the upstream head.

In this situation, a single head measurement at the throat region is sufficient to determine channel discharge. To measure the head, a stilling well is provided at the throat. Utilizing free flow discharge, the following expression is utilized to calculate the Venturi flume:

$$Q = 1.7 C_d B H^{3/2} \quad (2)$$

Where,  $C_d$  = Coefficient of discharge of Venturi flume

$B$  = width of the throat section

$H$  = Head measured in the stilling well.



Fig 1.2 Free Flow Flume

### 1.1.3. Parshall Flume

The Parshall flume is a variant of the venturi flume. The following alterations are performed to the venturi flume to shift the flow conditions from sub-critical to supercritical: increase in throat length, reduced angle of convergence of input walls , and reduced angle of divergence of outlet walls. The drop in elevation down the flume throat is a very important alternation. The Parshall flume can be designed as a free-flow parshall flume or as a submerged parshall flume, similar to the venturi flume.

#### 1.1.4. Cut throat Flume

A cut-throat flume is made up of a gradually contracting channel portion followed by a gradually increasing channel section. In the case of cut-throat flumes, the throat section is removed. A cut-throat flume has a flat and horizontal bottom surface. Building of cut throat flume is easier than other types of duct because it requires a level floor and flat sheet metal and does not require a throat section.



Fig No 1.3 Cut throat Flume

### 1.2 Necessity of Transition

Transition helps decrease loss in the head and ensure that the flow in the flumed portion is smooth without any unnecessary disturbances in flow upstream and downstream of transition. Where an unlined canal does not allow for a natural transition of flow, the vortices created at the entry and exit of the flumed section can cause a loss of total head, and an uneven distribution of both velocity and scouring. This requires the use of costly preventative measures. For instance, when a waterway is limited due to a bridge or an aqueduct to decrease the costs of constructing the bridge or the aqueduct, it is necessary to provide appropriate transitions at the beginning and end of the structure to decrease head losses and scour. A greater

reduction in head leads to greater inflow, causing several difficulties like sediment deposition and an uneven flow, resulting in extra preventive measures such as guide bunds, embankments, spurs and pitching. These protective measures are costly. Ensuring correct transitions will guarantee the flow in the flumed segment is maintained both within and outside the transitions. If adequate transitions are not planned in a hydropower plant's intake structure, there will be many difficulties, such as vibration and cavitations, which will damage the power plant's performance, including eventual failure or reduction in life and expensive maintenance costs. Suitable transitions at entrance and exit increase the performance of the structure, assuring improved efficiency and the elimination of unpleasant sediments that cause damage to the water conductor system, turbines, and diffusers.

### **1.3 Definition of Transition**

Transitions are necessary whenever a change in the cross-sectional area or shape of the canal is desired. Transitions are used to modify the shape of the main canal, and they made them up of short-length structural units. Fluming a trapezoidal canal into a rectangular canal in cross-drainage works, such as aqueducts, is a common instance of the need and application of transitions. There are other types of transitions, such as the entrance of a canal into a tunnel, the exit of a tunnel into a canal, and structures for cross-drainage like siphon aqueducts. When designing a transition for subcritical flows, the criteria should be to accomplish the necessary change in geometry with minimal disturbance to the flow and the most economical energy loss that is compatible with the project. The head loss produced is reflected by amplified upstream stages in this instance. Transitioning in a streamlined way decreases head loss, but it is costly; the cost is directly proportional to the level of streamlining. Swift and abrupt transitions are more financially sound, yet the energy depletion in the transition unit is very large. Therefore, a compromise must be reached between the shape of the transition and the cost of the transition. The design implemented in a subcritical transition thus becomes more specific to the location.

When a flow is supercritical, standing waves (Shocks) are generated a shift in the boundary's alignment, and the purpose of designing a transition in these flows is to

minimize the cross waves. The design is more complex than the transitions from subcritical to supercritical flow.

A transition is that portion (with varying cross-sections) of the channel that connects one prismatic channel to the other (which may or may not have the same cross-sectional form or dimensions). The variation in the channel section may result from changes in the breadth or the elevation or descent of the channel bottom. The two main types of channel transitions are abrupt and gradual transitions. Sudden transitions occur when the cross-sectional dimensions vary within a brief period. The change in the cross-sectional area happens gradually across a relatively long length of the channel, however, in the case of gradual transitions.

## **1.4 Classification of Transition**

Generally, flumes are divided into main two classes, which are described below

Class 1: Flumes with a free water surface that transition to an open channel are open to the atmosphere. With maximal pressure close to the bed, surface pressure is steady and roughly hydrostatically distributed along depth.

Class 2: Flumes with a closed conduit transition, such as confusers and diffusers, and a sealed water surface root are under pressure.

Class 1 open channel transition can be further subdivided into the following three groups as per the geometry of transitions

a. By adjusting the breadth without affecting the bed level, i.e. only modifying the horizontal planes. Venturi flumes, aqueduct transitions, and so on.

b. By modifying bed level without changing width, i.e. only in vertical planes, as with weirs, spillways, and so on.

c. By adjusting both bed width and bed level at the same time, i.e. in both horizontal and vertical planes. This category includes transitions in standing wave flumes, siphons, siphon aqueducts, and so on.

Class 1: Transitions are further classified based on flow regimes. Subcritical and supercritical flow in a channel, as follows:

(i) Transition from one subcritical flow to another subcritical as in aqueduct and siphon.



- (ii) Transition from subcritical to supercritical flow as in weirs and spillways
- (iii) Transition from supercritical to subcritical with a hydraulic jump as in energy dissipation structure
- (iv) Transition from supercritical to subcritical flow with no hydraulic jump, as in chutes

#### 1.4.1 Subcritical Flow Transition

The primary aspects that must be considered in the design of a transition include sharp angles in the structure that may cause energy loss. The resultant water surface from the transition should be a smooth, flat curve with no sudden shifts or standing waves. While numerous types of subcritical flow transitions are in use, the three types proposed by USACE are the most frequent.

These are the fundamental types.

- Cylindrical quadrant type, Fig. 1.4 (a)
- Warped type, Fig. 1.4 (b)
- Wedge type, Fig. 1.4 (c)

Each of these types is used in contractions as well as in expansions in subcritical flows.

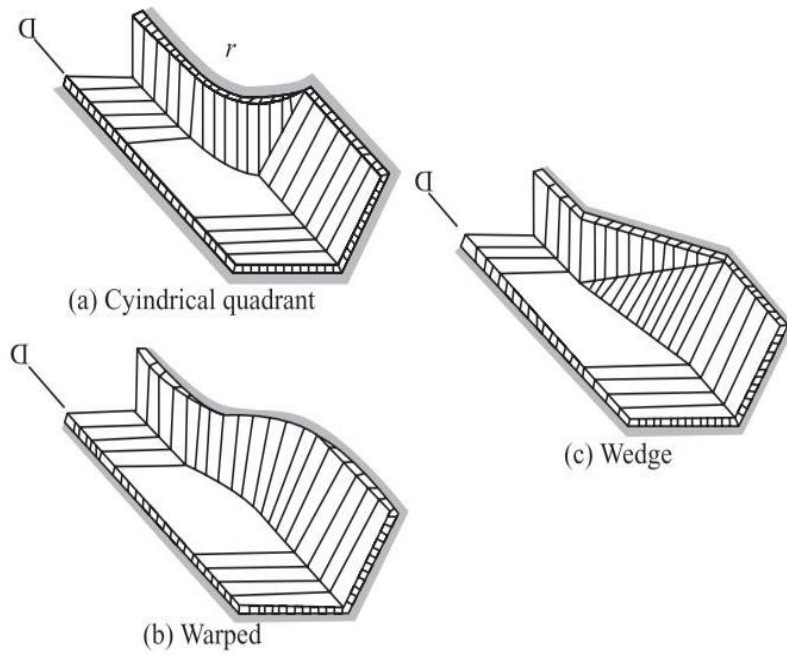


Fig 1.4 Basic Subcritical Flow transition types

#### Energy Equation for a Transition

There is a rise in speed when water passes through a section of constriction and the water level will lower in a subcritical flow. The energy line at the constricted segment will be lower than that at the upstream section due to energy loss during the contraction. The energy lost during contraction is indicated as a rise in the velocity head.

$$\Delta h_w = \left( \frac{V_d^2 - V_u^2}{2g} \right) \quad (3.1)$$

$$h_{ic} = C_c \left( \frac{V_d^2 - V_g^2}{2g} \right) = C_c \Delta h_{vc} \quad (3.2)$$

Where  $C_c$  = coefficient of energy loss at the contraction

The total energy relationship between two sections upstream and downstream of the constriction can be expressed as:

$$Z_u + y_u + \frac{V_u^2}{2g} = Z_d + y_d + \frac{V_d^2}{2g} + h_{ic}$$

$\Delta y'$  = change in the water surface elevation

$$\begin{aligned} &= (Z_u + y_u) - (Z_d + y_d) = \left( \frac{V_d^2}{2g} - \frac{V_u^2}{2g} \right) + C_c \left( \frac{V_d^2}{2g} - \frac{V_u^2}{2g} \right) \\ &= (1 + C_c) \left( \frac{V_d^2}{2g} - \frac{V_u^2}{2g} \right) = (1 + C_c) \Delta h_{ve} \end{aligned}$$

### Expansion

In an expansion, the velocity is lessened in the extended area, and subcritical flow, the water level increases. The energy line in the expanded area will be less than the energy line in the upstream region that is not extended.

The energy loss at the expansion is expressed in terms of the increase in the velocity head

$$\Delta h_e = \left( \frac{V_u^2 - V_d^2}{2g} \right) \quad (3.3)$$

$$h_{ie} = C_E \left( \frac{V_u^2 - V_d^2}{2g} \right) = C_E \Delta h_{ve} \quad (3.4)$$

Where  $C_E$  = coefficient of energy loss at the expansion.

The total energy relationship between two sections upstream and downstream of the expansion can be expressed as:

$$Z_u + y_u + \frac{V_u^2}{2g} = Z_d + y_d + \frac{V_d^2}{2g} + h_{ie}$$

$\Delta y'$  = rise in water surface elevation

$$\begin{aligned} &= (Z_d + y_d) - (Z_u + y_u) = \left( \frac{V_u^2}{2g} - \frac{V_d^2}{2g} \right) - C_E \left( \frac{V_u^2}{2g} - \frac{V_d^2}{2g} \right) \\ &= (1 - C_E) \left( \frac{V_u^2}{2g} - \frac{V_d^2}{2g} \right) = (1 - C_E) \Delta h_{vc} \end{aligned} \quad (3.5)$$

**Table no. 1: Transition Loss Coefficient**

S.No	Shape of Transition	$C_c$	$C_E$
1	Warped Type	0.1	0.2
2	Straight ended/abrupt	0.3	0.75
3	Straight line	0.3	0.3
4	Cylinder Quadrant type	0.15	0.25
5	Wedge type	0.2	0.3

## 1.5 General Features of Various Transition Types

### 1.5.1 Warped Types

The goal of the warped transition is to provide the most hydraulically efficient transition between the two canal sections. As a result, the transition loss coefficients  $C_c$  and  $C_E$  for this kind are the smallest, with average values of 0.10 and 0.20, respectively. These structures, however, are too expensive. There are numerous empirical methodologies accessible for design. It is common practise to preserve the expansion angle  $\theta$ , defined as

$$\theta = \tan^{-1} \left[ \frac{\text{Difference in top width}}{2 \times \text{length of the transition}} \right] \quad (3.5)$$

at a value  $\leq 22.5^\circ$ . Warped-type transition is recommended in significant canal construction where energy losses must be kept to a minimum.

### 1.5.2 Cylindrical Quadrant Type

The United States Department of Agriculture (USDA) crafted this design as a cost-effective alternative to expensive warped transitions. At the endpoints of the transition, it is composed of two cylindrical quadrant vertical walls that connect the two channels. The difference in top widths of the connected channels is divided by two to get the quadrant's radius. These are used for transitions from rectangular to rectangular, rectangular to trapezoidal, and trapezoidal to rectangular channel shapes. The expansion loss coefficient  $C_E$  is identical to the warped transition of 0.20, and the contraction loss coefficient  $C_C$  is nearly as good as the warped design of 0.20.

### 1.5.3 Wedge Type

This design is a simplified wedge type for ease of design and production. Straight-edge mitre pieces affect the design. Figure 1.5 displays the technicalities of constructing the wedge forms for the bed as well as the sides in a rectangular to trapezoidal transition. While the wedge-type design is less expensive than a warped transition, it is inefficient hydraulically. Hydraulic efficiency is higher for the cylindrical quadrant type than the wedge type. The expansion angle  $\theta$  is to be kept at not greater than 22 for expansions and not greater than 27.5 for contractions.

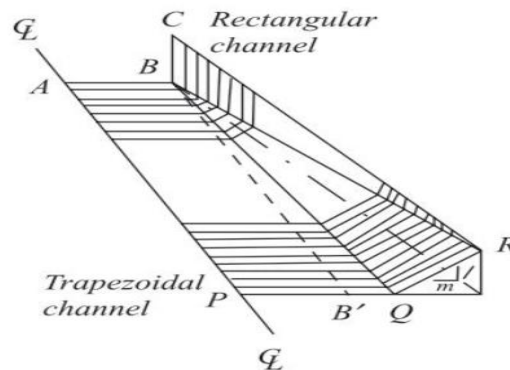


Figure 1.5 Wedge-type Transition from rectangular to trapezoidal channel

## 1.6 ECONOMICS OF TRANSITION

It is not always required to provide transition where fluming is very high. Mostly transition are required where the overall cost of the flumed structure and transition is minimum. Consequently, a financial examination should be conducted to determine the amount of fluming to be done to guarantee the most minimal total expense of the flumed structure and the transitions. For instance, flumming of a trapezoidal and then canal is required with the following goals when an aqueduct is to be built to transport the canal across a broad river. The first objective is to reduce the cost of the concrete flume. The goal is to attach the trapezoidal section of the earthen canal to either a metal/concrete pipe that carries the canal's water over the river or a rectangular trough, depending on the magnitude of the flow.

If the flow of the flume is too strong and suitable transitions are not provided for entry and exit points. Upstreams will experience influx, backflow and sedimentation, while downstream will undergo scouring. After that, if the stream is a small one, it may be more economical to construct the canal in its natural earthen section and build an inverted siphon aqueduct to have the stream pass underneath the canal.

Analyzing the situation, it is more cost-effective to use a flume to channel the natural flow of the stream and decrease the cost of transporting the stream flow. Different forms of cross-drainage configurations are given with transitions where necessary, depending on the relative size of the canal and the stream, as well as the difference in their beds and water levels. If both the stream and the canal can be flumed economically. Four sets of transitions will thus be required—two for the canal and two for the stream.

Similarly, when building a bridge over a river that flows through extensive flood plains, it is typical to flume the river by installing guide bands to minimise the bridge span for the economy. Guide bunds are structures that connect the bridge opening to the usual river segment. According to Mazumder et al. (2002), restricting the flood plain too much causes several issues, including hydraulic jump formation, river bed scouring, and flow choking that results in extremely high afflux upstream. Due to siltation, which has caused the river to broaden and outflank the bridge, the river may

be unstable upstream (Mazumder, 2010). Without a sufficient transition structure for proper diffusion flow, the river's bed and banks will be worn away by high-velocity flow, resulting in costly foundation and protective works for the river and its environments.

Approach embankments connect the bridge to the road. Bradley (1970) thoroughly investigated the relative economics of river fluming.

Comprehensive research on guiding bunds with elliptical-type transitions was done by Laggase et al. in 1995. An example has been developed to demonstrate the design of the guide banks for a bridge across the Yamuna river.

Like bridges, inlet and outlet transitions are frequently utilised in road culverts to decrease head loss and afflux and enhance culvert carrying capacity. Diffusion of flow at culvert exits to reduce scour and the expense of protective mea

## CHAPTER 2

### REVIEW OF LITERATURE

#### 2.1 LITERATURE REVIEW

**Sihag et al. (2021)** conducted model establishment and validation of aeration efficiency with Modified Venturi flume and Parshall flumes were used. It was done by conducting experiments for different Venturi flumes and one Parshall flume. The model produces a training dataset that included 70 observations, while they considered the remaining observations in the model for validation test. They choose various independent variables which were considered for inputs are throat width , flow rate, sill height, throat lengths, oxygen deficit ratio, and exponent, while aeration efficiency was observed. From the result, it was concluded that oxygen deficit was the most effective input parameter for estimating aeration efficiency.

**Heyrani (2021) et al.** performed a experiment in a rectangular channel to assess the variations in the amount of dissolved oxygen in the stream prior to and after a Parshall flume structure was implemented. He used the dimensions of the Parshall flumes in the research as the 3-inch with a 45-degree wing wall. An analysis of various turbulence models, such as the standard k-epsilon, realizable k-epsilon, RNG k-epsilon, k-w SST, k-w SST DES, Smagorinsky, and the dynamic K LES, demonstrated that even though k-w SST was not as successful within two cross-sections as the other models apart from DES family models, it was still able to accurately estimate the water level.

**Sun et al (2021)** conducted a number of experiments and performed numerical analysis on the cutthroat flume, NACA airfoil-shaped flume, airfoil pillar-shaped flume, and optimized airfoil-shaped flume in rectangular channels. Three different contraction ratios of 0.4, 0.5 and 0.6 were implemented in the rectangular channel. Upstream Froude number was least in the case of air shaped flume .



**Sun, Yang et al. (2020)** performed experiments on a portable pillar-shaped flume with three contraction ratios under various working conditions. The numerical simulations and experiments were merged in order to create the theoretical stage-discharge formula of the movable pillar-shaped flume. An examination of the discrepancies in the Froude number, backwater height, critical submergence, head loss, and velocity distribution was carried out. The upstream Froude number was less than 0.5 and the critical submergence was between 0.73 and 0.96, fulfilling the necessary conditions. Compared to the airfoil pillar-shaped flumes, the portable pillar-shaped flume had a much lower head loss and backwater height.

**Zuikov (2019) et al** discovered a functional relationship between the Froude number and any chosen segment of the Venturi channel, and the breadth of the critical section..It was discovered that the flow was unstable within a rectilinear gorge region of a Venturi channel, which is connected to the proximity of its parameters to the critical ones. The optimization approach of a profile of a Venturi channel with a dividing cross-section in a gorge without empirical coefficients is considered. They offered a technique that allows for the assessment of the main geometric measurements and hydraulic properties of the Venturi flume, such as its flow rate coefficient, the arrangement of depths and flow velocities throughout the flume's length.

**Zuikov (2018) et al** discovered a theoretical method of hydraulic calculation of the full-capacity discharge of the Venturi channel, which does not contain empirical coefficients. It was postulated that in a classical Venturi flume with an unrestricted liquid outflow, regardless of the flow rate, the flow will pass a significant depth within the ravine part with vertical sides in alignment. The position of the critical section was in the middle of the gorge section. The critical section in proximity to the diffuser is subject to an increase in discharge. In the upstream area of the Venturi flume and its convergence, the flow is tranquil and below the critical level, while in the middle section of the flume gorge, the flow is at a critical level irrespective of the rate of flow, and is supercritical in the diffuser. The specific energy of the flow in the upstream pool to the water level in it is represented by the ratio  $E/h$ , which is solely

determined by the ratio of the width of the Venturi flume's gorge to the width of the upstream channel  $b/B$ .

**Castor Orgaz et.al. (2018)** employed a critical theory on an open channel of a curvilinear plane to take into consideration the curvilinear flow effects of a streamlined flow with a round arc entrance. He developed critical flow theory and broadened the use of a former lower-order theory from  $U = 0.5$  to  $U = 4$ . He has put forward a fundamental design method for the Khafagi flume. He had established novel criteria for the computation of throat length, i.e.  $L_t = 0.2 H_d$ .

**Zerihun (2016)** conducted a study on a model with a single dimension that includes a dynamic pressure modification of a higher order to factor in the effect of the sidewalls. Such flows were simulated using streamline vertical curvatures, which also helped to highlight important flow characteristics. The model equations were divided into discrete pieces and solved utilizing the finite difference scheme. The model was put into use to with a contraction ratio ranging from 0.38 to 0.62, short-throated flumes can be used to imitate the key features of curvilinear flows. The measured values were compared to free surface profiles, pressure distributions at various sections, and discharge characteristics. The developed model could accurately simulate the curvilinear flows in short-throated flumes with rounded transitions and bottom humps. The results also demonstrate the intricate relationship between the discharge properties of the critical-flow flumes under free-flow conditions and the curvature of the streamlines.

**Dufresne et al.(2013)** study concentrates on ascertaining the head–discharge relationship for Venturi flumes employed for flow discharge measurements in open channels. Dimensional analysis was used to highlight the five dimensionless variables can that influence the discharge coefficient  $C_{D2}$ , Namely the ratio of the breadth of the approach channel to the breadth of the throat  $B/B_t$ , the dimensionless energy head  $H/B_t$ , the dimensionless length of the throat  $L_t/B_t$ , the dimensionless

radius of curvature of the arc-shaped convergence  $R/Bt$  and the outlet expansion ratio  $(B - Bt)/(2Le)$ . They extended the limitation of the traditional critical flow theory to a ratio of the energy head to the length of the throat up to 1.0 and proposed an equation for the discharge coefficient, which is valid for an 8 % deviation. Dimensionless lengths were applied from 0.2 to 3.0 and dimensionless radius of curvature from 1.0 to 4.0. The width ratio of 2.0 and an expansion ratio of 1:6 are used in the research,

**T. Gill et al. (2006)** made use of a submerged venturi flume to assess the examining the capability of accurately measuring approach sections and throat depths. The test model featured a trapezoidal channel with a flat bottom width and 1:1 side slopes. The throat segment has a length in the direction of flow of 3 feet and a bottom width of 0.333 feet with side slopes of 1:1. Each portion of the throat's gradual contraction and expansion in the flow direction is 3 feet long, maintaining a uniform side slope. At the downstream end of the channel, a long-throated flume was built to measure the control flow as well as to submerge the venturi flume.

**Emiroglu et al (2003)** explored the air entrainment rate and oxygen transfer efficiency of venturi devices with air holes running along the length of its convergent-divergent passage in an experiment. Results indicated that the air entrainment rate and oxygen transfer efficiency of the venturi device were notably higher compared to that of the circular nozzle. The oxygen transfer efficiency at low water jet velocities was very high. This can be attributed to the decrease in bubble penetration depth at low water jet velocities.

**Wright et.al. (1991)** used a numerical models to develop an alternative rating equation at a low flow rate for a Parshall flume of different sizes. He concluded that Parshall's original equations were valid for high discharges but overpredict for low discharges.

## **CHAPTER 3**

### **MATERIALS AND METHODOLOGY**

#### **3.1 OBJECTIVE OF THE PRESENT STUDY**

- 1.To determine the Froude number for different width ratios of venturi flume
- 2.To plot the specific energy curve for various discharges and width ratio
- 3.To plot flow profile for different discharges and width ratio
4. To optimize of width of flume based on Froude number and flow condition

### 3.2 Model

Three distinct models are utilized with varying throat lengths and the models are composed of steel. The model is constructed with a converging ratio of 1:4 and an expansion ratio of 1:6, and the width of the flume alternates between 25 cm and 20 cm and 18 cm. The section of expansion region is always larger than the converging section.



Figure 3.1.: Model 1 with width ratio (0.5)



Figure 3.2: Model 2 with width ratio (0.4)



Figure 3.3 : Model 3 with width ratio 0.36.

### 3.3 EXPERIMENTAL SETUP

A specific experimental facility has been built in the “Fluid Mechanics and Hydraulics Research Laboratory” at Delhi Technological University, Delhi, India, to perform all the scale model tests depicted hereafter. A straight rectangular channel, 10 m long, 0.6 m deep, and 0.50 m wide, has been used to carry out a range of scale model tests depicted hereafter. A series of pipes of a 4-inch supply coupled to a 20.0 Horse Power (HP) pump is used to feed the channel, providing discharges up to a value of 50 L/s.. The supply line of the flume is calibrated using an orifice meter (having an uncertainty of 0.25%) along with a flow-regulating valve to control the discharge. A 4-20mA electromagnetic flowmeter (uncertainty  $\pm 0.2\%$ ) is fitted with a supply pipe for the discharge measurement. In addition, the flume is fitted with a 4-20 mA ultrasonic level sensor (with an accuracy of  $\pm 0.2\% \pm 1\text{ mm}$ ) instrumentation carriage and a pointer gauge of least count  $\pm 0.1\text{ mm}$ , which are utilized to measure the height of the water surface and crest elevations in various sections. The different model of venturi flume is placed at the 6m from the screen gate. The reading is taken at the two points of the venturi flume one at the starting and the other at the throat section of the venturiflume.

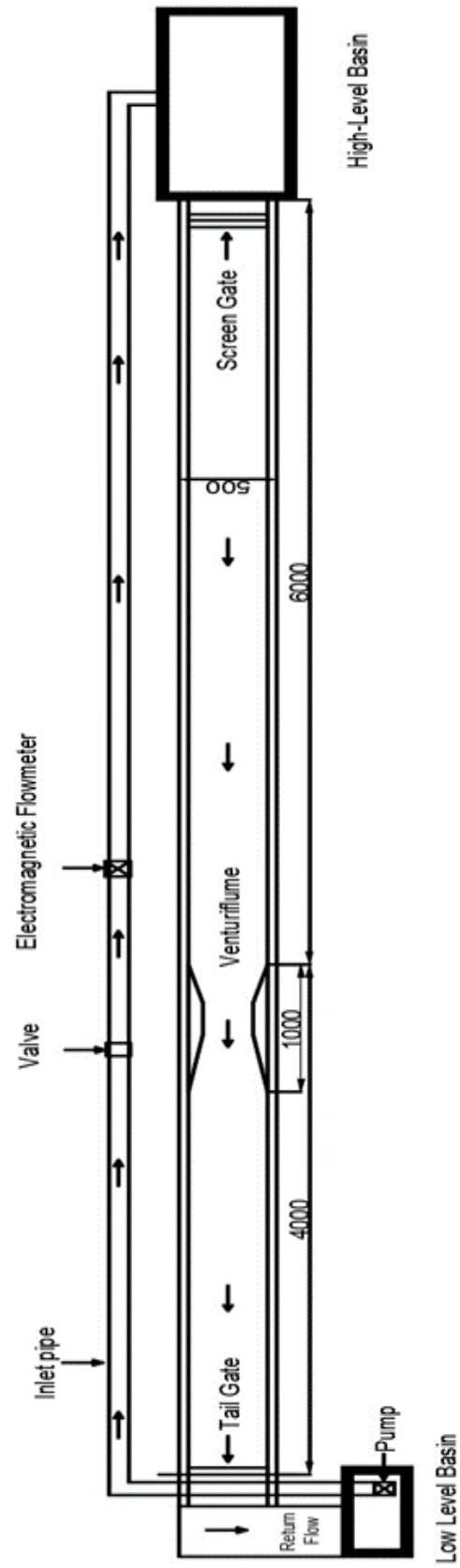


Figure 3.4 Experimental Setup (All dimensions in mm)

## 3.4 TOOLS AND INSTRUMENTATION

### 3.4.1 Digital Manometer

This Digital Manometer features a wide pressure range of 10 psi, making it suitable for use in many industrial uses. It features double-lined scales and can easily connect to external vacuum or pressure sources via a 1/8 "NPT connector. This digital pressure gauge is economical and gets the job done. The Manometer has two sensors that make it possible to measure two different pressures at one time. Each sensor has a male BSPP thread with a 0-160 psi range or 50 kPa range. It comes featured with an intuitive LCD that shows the readings in an easy-to-read format. The instrument comes with a 9V battery only and can handle temperatures from -20°C to 120°C.

The digital measuring instrument is used for checking the pressure of tanks, pipes, compressed air and other fluids. It had been designed to withstand extremely high pressures, making it ideal for use in the laboratory. It is also different in that it has no mercury, which means there is no risk of mercury poisoning.



Figure 3.5: Digital Manometer

### Working Principle of Digital Manometer and Pitot Tube

Henri Pitot used a bent glass tube to measure river velocity in France in the 1700s, and this is how the Pitot tube got its name. Pitot tubes are fairly straightforward instruments that monitor flow velocities and have no moving parts. A typical style of insertion flowmeter is a pitot tube. The reference pressure (or static pressure) in the pipe is compared to this "velocity" pressure, and the velocity may be calculated by



using a straightforward equation. Pitot tubes are two hollow tubes that are used to gauge pressure in various locations along a pipe. The other tube is used to monitor simply the static pressure, typically near the pipe wall, while the first tube measures the impact or stagnation pressure. These tubes can be put individually in a pipe or collectively in a single casing to form a single device.

A Pitot tube, a cylindrical device with one end open and the other end closed, is a simple tool. When fluid travels through a pipeline, it enters and comes to a stop in the Pitot tube. The difference between two pressures is used to calculate the dynamic pressure. The dynamic pressure is calculated by determining the difference in height between the liquid in the tube and the free surface. As with other instruments, the flow rate is determined by taking the square root of pressure. However, the accuracy of the estimation of the flow rate is affected by the design of the tube and the location of the static tap. To eliminate this effect, static holes are included in the Pitot-static probe's tube system. The static pressure and impact pressure are then linked to the appropriate differential pressure meter, which is used to determine flow velocity and subsequently flow rate.

$$v = \sqrt{\frac{2\Delta p}{\rho}} \quad (3.1)$$

$\Delta p$  = differential pressure in kPa

$\rho$  = density of water in kg/m<sup>3</sup>

$v$  = velocity in m/s

The velocity is taken at the three point in the tranverse direction and five point in the vertical direction. Then by the method of depth-averaged and the velocity at the 0.6 y from the top of the water surface.

### 3.4.2 Electromagnetic flowmeter

Electromagnetic Flow Meter is a volumetric flow meter that is typically employed in applications involving waste water , systems with a low drop in pressure, while also necessitating appropriate liquid conductivity .This device has no moving parts and is not compatible with distilled water and hydrocarbons. Mag flow metres require

little upkeep as well. On the basis of Faraday's Law of Electromagnetic magnetic flow metres function. A voltage  $E$  is generated when a medium that conducts passes through a magnetic field, according to this idea. The velocity of the medium, the density of magnetic field, and the length of conductor are all proportional to this.

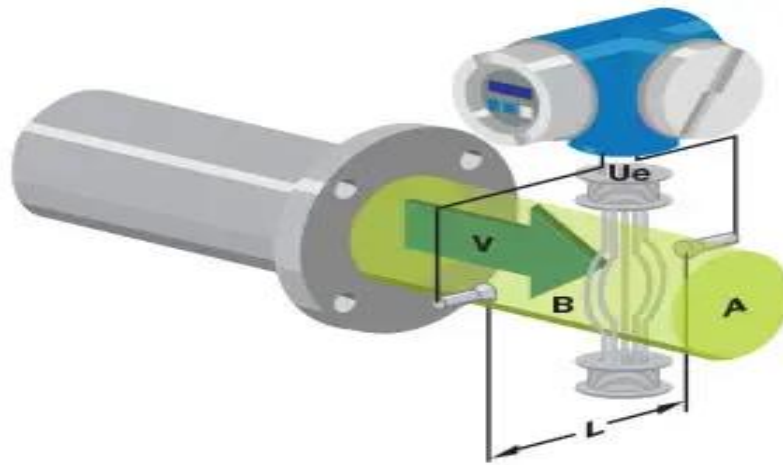


Figure 3.6 Diagram of Electromagnetic flowmeter

A magnetic field is created in a magnetic flow metre by applying a current to wire coils positioned inside or outside the metre body. A voltage is produced that is proportionate to the average flow velocity by the liquid acting as the conductor in the pipe. Sensing electrodes built inside the Magflow metre body detect this voltage, which is then transmitted to a transmitter that uses the pipe dimensions to determine the volumetric flow rate. Faraday's law can be expressed mathematically as  $E$  is proportional to  $V \times B \times L$  [ $E$  is the voltage created in a conductor,  $V$  is the conductor's velocity,  $B$  is the strength of the magnetic field, and  $L$  is the conductor's length]. The liquid flow that will be monitored by the magnetic flow metre must be electrically conductive, which is crucial. According to Faraday's Law, the signal voltage ( $E$ ) is influenced by the average liquid velocity ( $V$ ), conductor length ( $D$ ), and magnetic field intensity ( $B$ ). Thus, the magnetic field will be created in the tube's cross-section.

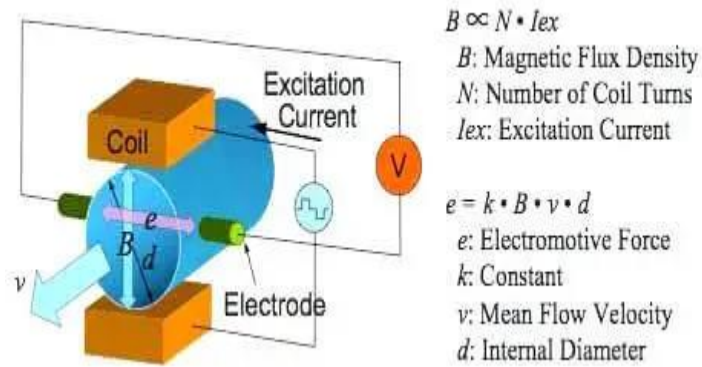


Figure 3.7 Schematic diagram of electromagnetic flowmeter

This type of metre can be used to measure heavy suspensions like mud, sewage, and wood pulp because there is essentially no flow obstruction. Other than the pressure head loss caused by the length of straight pipe the flow metre occupies, there is no pressure head loss in this kind of flow metre. The disturbances in the upstream flow have little impact on them. Variations in density, viscosity, pressure, and temperature have almost no impact on them. Low (15 or 20 W) electrical power requirements are possible, especially with pulsed DC types.

These metres are capable of being used in both directions. The chosen lining materials for the metres' interiors are not only excellent electrical insulators but also corrosion resistant, making them appropriate for the majority of acids, bases, water, and aqueous solutions. In addition to being less obstructive, the metres are frequently used for slurry services because some of the liners, like neoprene, and rubber, have strong abrasive resistance. They can handle very low flows.

This electromagnetic flow meter can accommodate any fluid that has an electrical conductivity above 10 micro siemens/cm due to its unobtrusive design. Its versatility allows it to measure a variety of fluids, such as sand water slurry, coal. It also has the capability to measure hot fluids, high viscosity fluids, particularly in the food processing industry, and even cryogenic fluids.

### 3.5 Methodology

A specific experimental facility has been built in the “Fluid and Hydraulics Research Laboratory” at Delhi Technological University, Delhi, India, to perform all the model tests. The flume with the rectangular channel, 10 m long, 0.6 m deep, and 0.50 m wide, has been used. A venturi flume model was prepared in which the converging ratio (1:4 ) and the diverging ratio (1:6).

The experiment are conducted for 3 different throat widths of 25cm, 20 cm, and 18 cm and 5 different discharges vary from 20 l/s to 40 l/s.in the increment of 5 l/s. The supply line of the flume is calibrated using an orifice meter (having an uncertainty of 0.25%) along with a flow-regulating valve to control the discharge. The discharges are taken from the electromagnetic flowmeter (uncertainty  $\pm 0.2\%$ ). Venturiflume are glued to the sides of the channel with clay so that they are not affected by any fluctuations. Initially water will be allowed to enter the flume gently and when the entire flume is wetted The flow can then go into the sink as the flow starts to require a steady state.

The depth of water flow will be maintained with the help of a tailgate, which marks the start of the run time, which lasts up to 15 minutes and measures the velocity with the help of a static pitot tube. The head is measured with the help of a point gauge, velocity will be measured at the upstream and throat of the venturi flume. The velocity is taken at the three points in the transverse direction and five points in the vertical direction. Then by the method of depth-averaged and the velocity at the 0.6 y from the top of the water surface. Velocity is measured in two sections, first at the entry of the venturi flume and another section at the throat of the venturi flume.

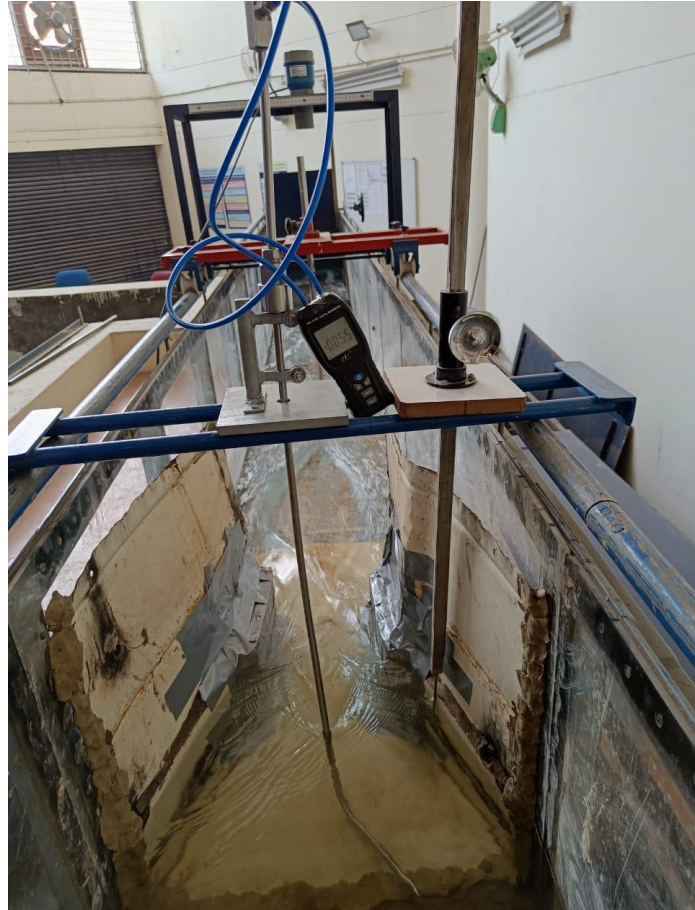


Figure 3.8 Measurement of Velocity with the help of pitot tube



Figure 3.9 Measurement of depth

The plot of the water surface profile is done by taking reading 17 points across the venturiflume. Three points are before the venturing flume , three points at the converging section , five points at the throat section from (300mm to 550 mm ) , four points in the diverging section and two points ater the diverging section .

These steps are again repeated for three discharges 40 l/s, 30l/s and 20l/s for the different width ratio.

## CHAPTER - 4

### RESULTS AND DISCUSSION

#### 4.1 Effect of Specific energy for various width ratio

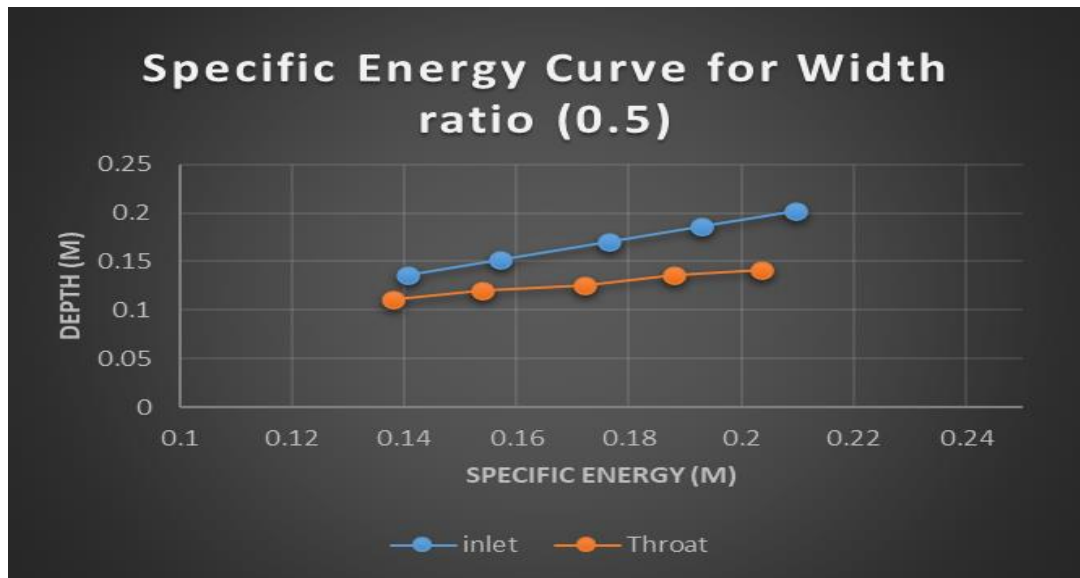


Figure 4.1 Specific Energy curve for width ratio (0.5)

The above plot shows the specific energy curve for the width ratio 0.5, for various discharges varies from 20 l/s to 40 l/s at an increment of 5 l/s and thus corresponding depth have been plotted in y axis. The Specific energy are more at the high than the low discharge. At the low discharges the depth at throat and inlet has a very less difference.

From the Figure no. 4.2 and Figure no 4.3, the difference between the specific energy at the low discharges are more than that of the width ratio (0.5).

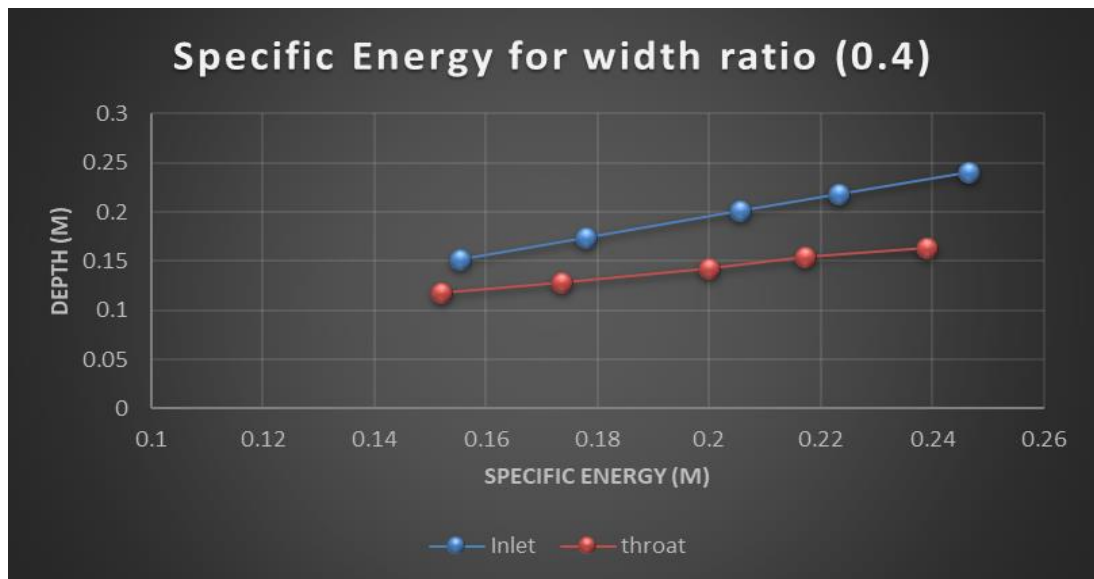


Figure 4.2 Specific Energy curve for width ratio (0.4)

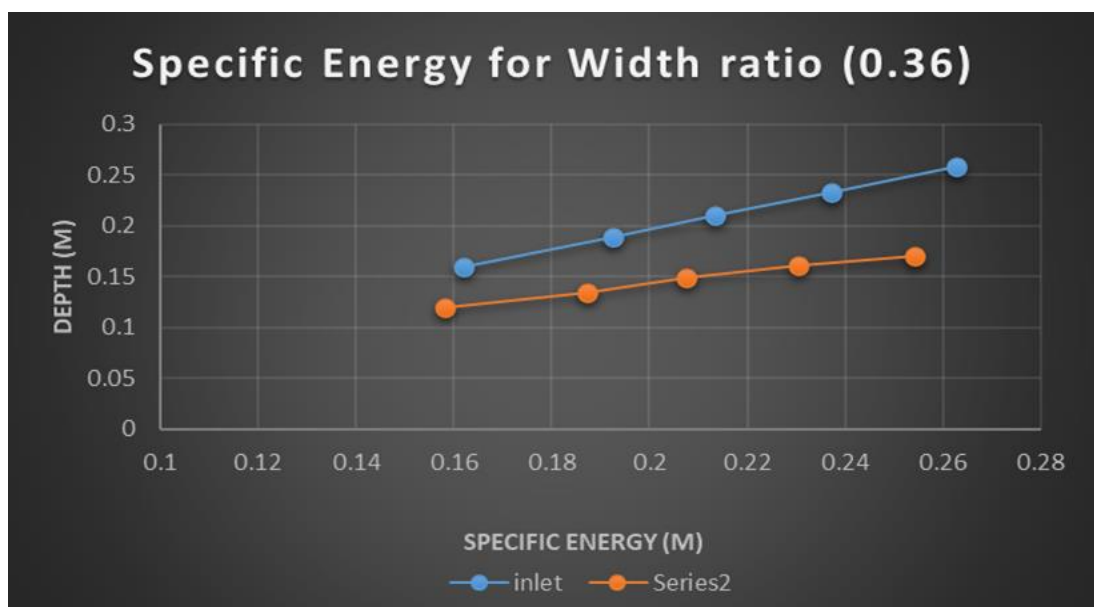


Fig 4.3 Specific Energy curve for the width ratio (0.36)

The specific energy at the inlet is higher than the throat due to the losses are higher in the throat section. For the decrement of the width ratio from 0.5 to 0.36 . As the value of discharges is increasing the difference in between them also increases.

In Fig 4.1, the specific energy at the throat for the width ratio (0.5) is less than the other two width ratio , As the section becoming critical at the throat ,after that the structure become costly and there form a supercritical transition.



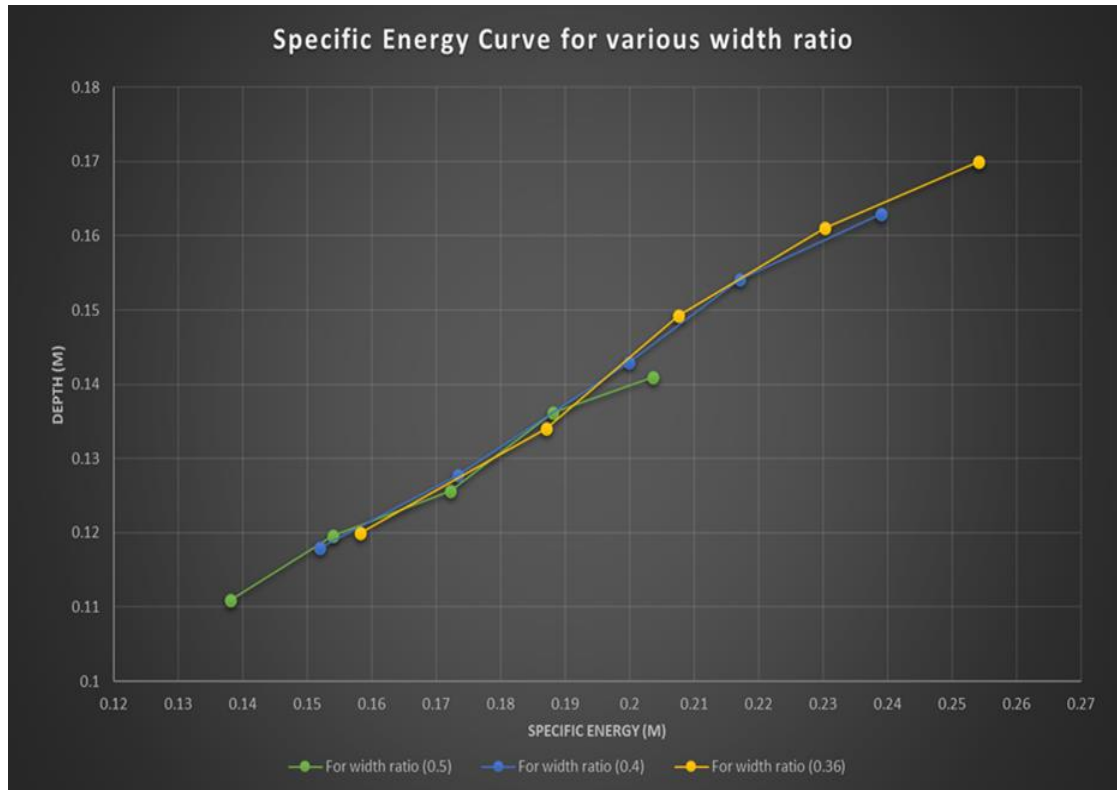


Figure 4.4 Specific Energy curve for various width ratio

This curve is very interesting and give unique finding as the specific energy curve at the throat for the venturiflume move upwards when the decrement of the width ratio. As the section became contracted , the energy at the throat section is more as its depth is also increasing .

Table no.2 .3 and 4 represent the reading taken while performing the experiment .Initially the discharge is set then the other variables are measured. Velocity is also checked by the depth averaged method , Here  $h_1$  and  $h_2$  represent the depth measured at the inlet and throat respectively

**Table no 2 Reading for the experiment for width ratio (0.5)**

h1 (m)	h2 (m)	Q (m <sup>3</sup> /s)	v1 (m/s)	F1	v2 (m/s)	F2	E1(m)	E2 (m)	del E
0.202	0.141	0.040	0.3870	0.275	1.109	0.942	0.2096	0.2036	0.00595
0.186	0.1362	0.035	0.3694	0.274	1.009	0.873	0.1929	0.1881	0.00485
0.1702	0.1256	0.030	0.3527	0.273	0.956	0.861	0.1765	0.1721	0.00435
0.1518	0.11965	0.025	0.3235	0.265	0.820	0.758	0.1571	0.1540	0.00313
0.136	0.111	0.020	0.2974	0.257	0.728	0.698	0.1405	0.1380	0.00244

**Table no 3 Reading for the experiment for width ratio ( 0.4)**

h1(m)	h2 (m)	Q(m <sup>3</sup> /s)	v1 (m/s)	F1	v2(m/s)	F2	E1 (m)	E2 (m)	del E
0.241	0.163	0.040	0.3302	0.2147	1.22	0.9653	0.2465	0.2389	0.00761
0.2183	0.1542	0.035	0.3138	0.2144	1.11	0.9030	0.2233	0.2170	0.00625
0.201	0.143	0.030	0.3008	0.2142	1.05	0.8925	0.2056	0.1999	0.00566
0.174	0.1278	0.025	0.2779	0.2127	0.94	0.8450	0.1779	0.1734	0.0045
0.152	0.118	0.020	0.2534	0.2075	0.816	0.7586	0.1552	0.1519	0.00332

**Table no 4 Reading for the for experiment width ratio ( 0.36)**

h1 (m)	h2 (m)	Q(m <sup>3</sup> /s)	v1 (m/s)	F1	V2 (m/s)	F2	E1 (m)	E2 (m)	del E
0.258	0.17	0.04	0.304	0.1915	1.2849	0.9950	0.2627	0.254	0.00858
0.233	0.1611	0.035	0.289	0.1918	1.165	0.9267	0.2372	0.2303	0.00701
0.2096	0.1493	0.030	0.274	0.192	1.0690	0.8834	0.2134	0.2075	0.00587

0.189	0.1341	0.025	0.260	0.1913	1.0197	0.8891	0.19246	0.1871	0.00535
0.1593	0.12	0.020	0.235	0.1880	0.8666	0.7987	0.1622	0.1582	0.00383

#### 4.2 Variation of Froude Number with various width ratio

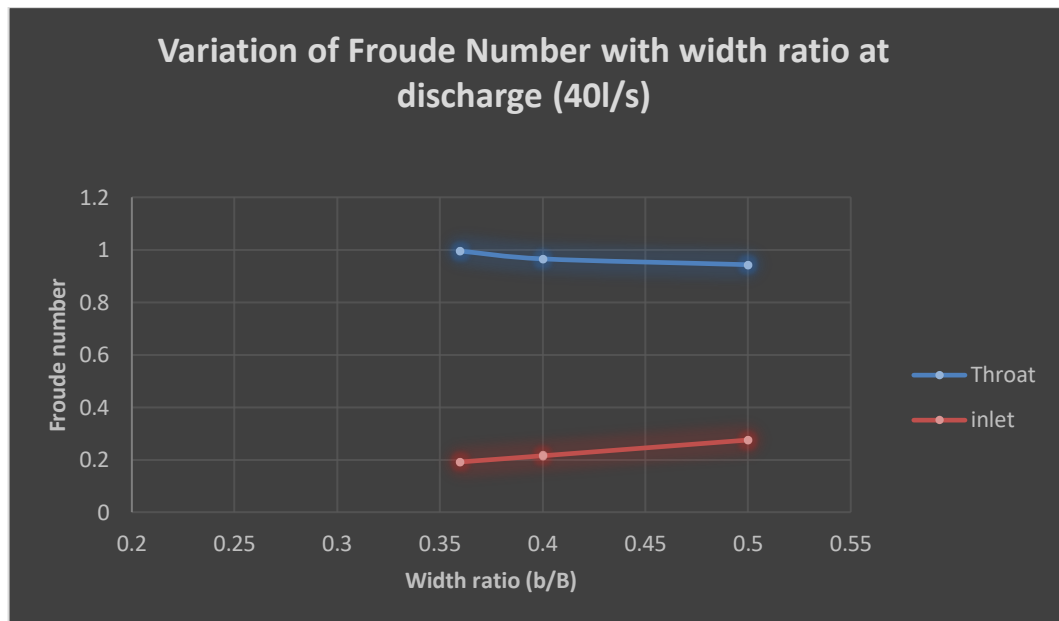


Figure 4.5 Variation of Froude number with width ratio at discharge (40l/s)

In the Fig 4.5 ,the Froude number increases at the inlet with an increment of the width ratio. The Froude number increases from 0.19 to 0.28 up to the critical when the width ratio changes from 0.5 to 0.36. After this the critical section made in the throat and section became costlier.

In the Fig 4.6 ,the Froude number changes from 0.87 to 0.92 when we change the width ratio from 0.5 to 0.36 , It is interesting to observe that the as the discharges getting reduced Froude number decreases .

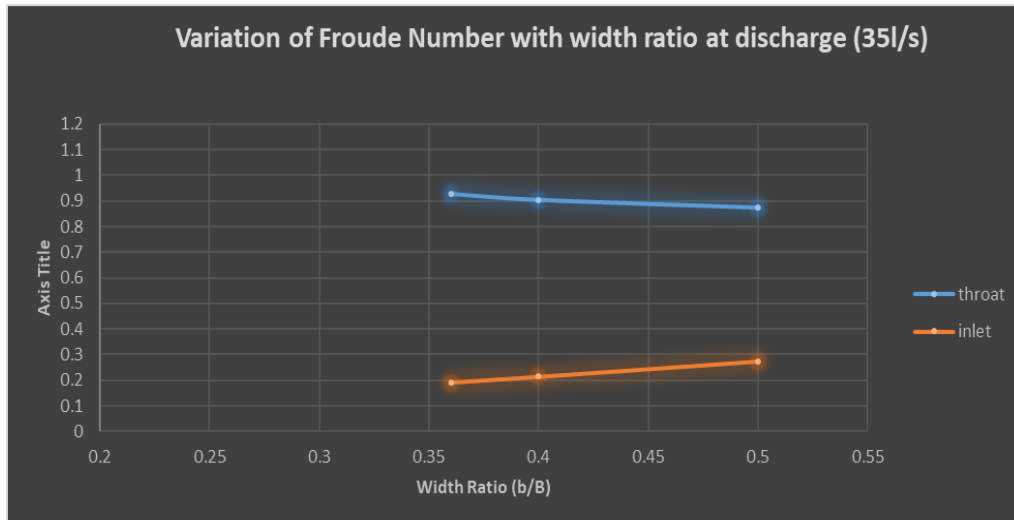


Figure 4.6 Variation of Froude number with width ratio at discharge (35l/s)

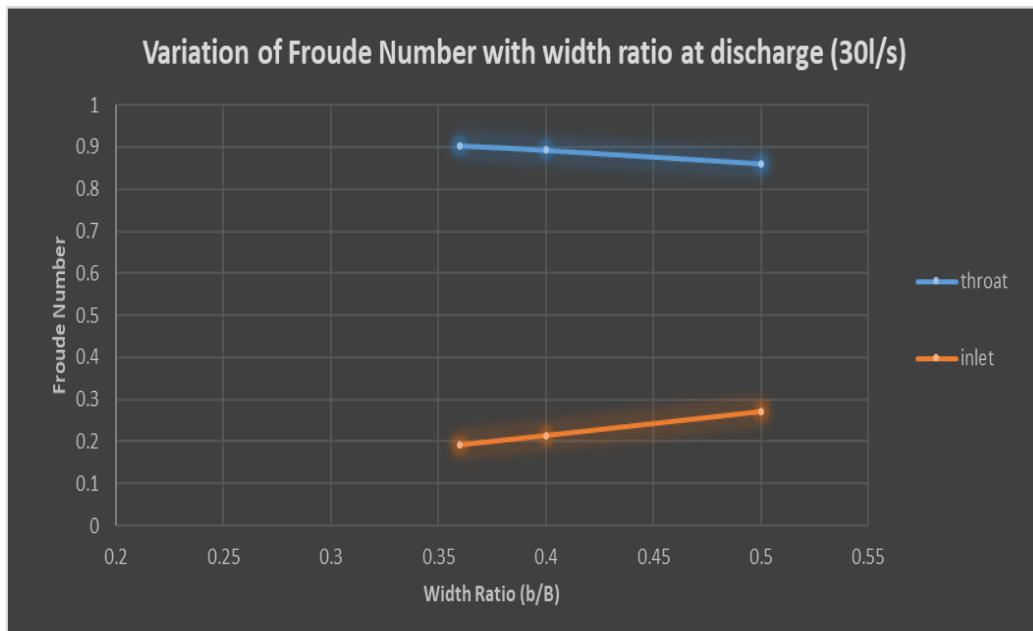


Figure 4.7 Variation of Froude number with width ratio at discharge (30l/s)

In the Figure 4.6 , the Froude number varies from 0.86 to 0.926 with the decrement of the width ratio from 0.5 to 0.36. Also in the Figure 4.7 , the Froude number changes from 0.861 to 0.903 , as the width ratio decreases .

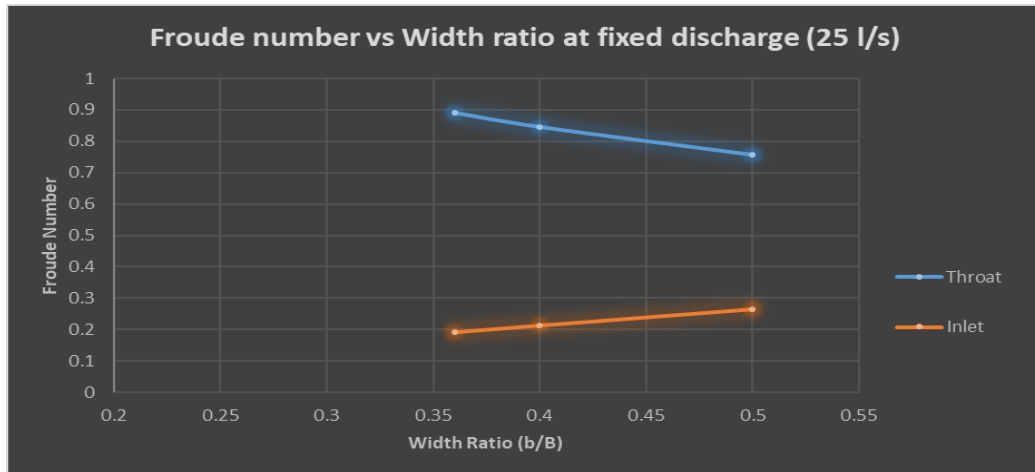


Figure 4.8 Variation of Froude number with width ratio at discharge (25l/s)

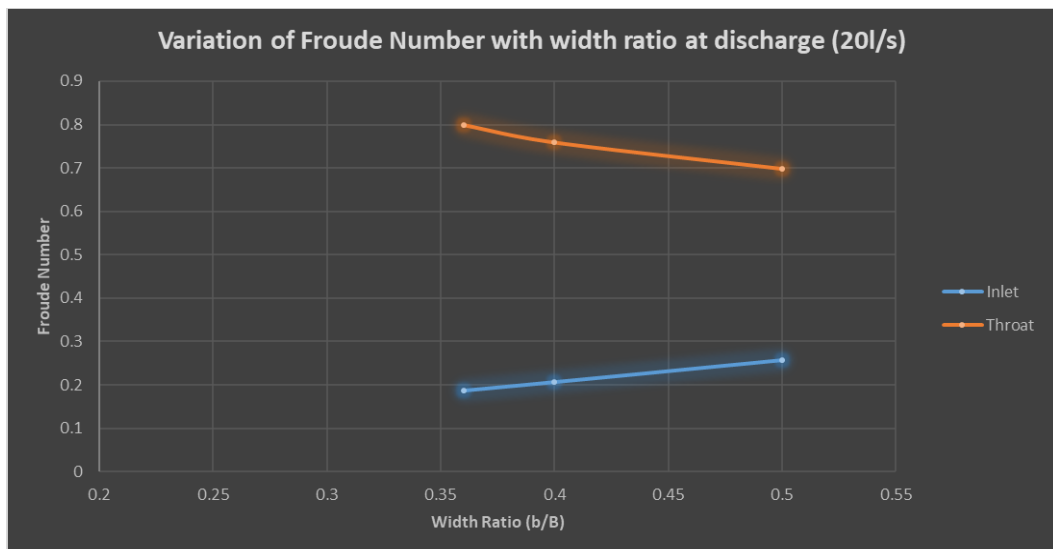


Figure 4.9 Variation of Froude number with width ratio at discharge (20l/s)

The Froude number changes from 0.75 to 0.88 for the discharge 25l/s (Figure 4.8 ) and the froude number drastically varied from 0.698 to 0.7987 for the discharges 20 l/s ( Figure no 4.9). Therefore, for the low discharges the Froude number drastically changes but for the the high discharges the Froude increases in a quick succession.

### 4.3 Variation of Froude number and Discharge

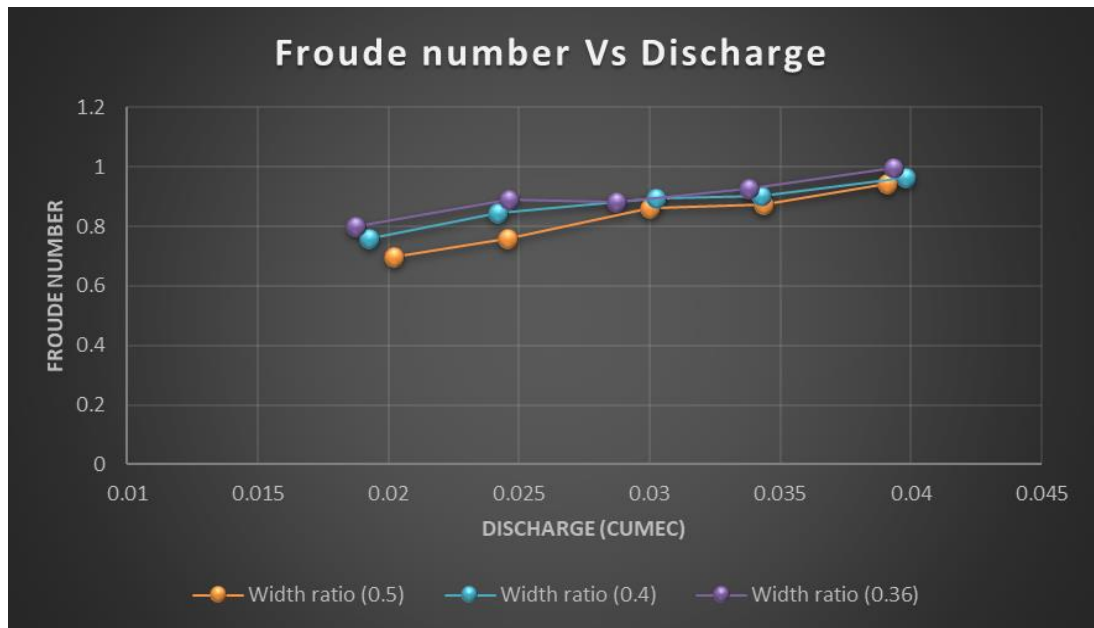


Figure 4.10 Variation of Froude Number and discharge

The Froude number is found to be increasing when the discharge is increasing. But it is interesting to see that the width ratio is decreasing but the Froude number at the throat section is going to critical. At the low discharges the Froude number is different but as we are going towards the high discharges the Froude number increases rapidly.

#### 4.4 Plot of water surface profile for different width ratio

The water surface profile are plotted with 2 points before the inlet , 0 to 30 cm is the converging section of the venturiflume, And the section after the 30 cm to 45 cm in the flow direction is the mid of the throat where we observed the reading of the throat .The plot is plotted for all the width ratio with three different discharges 40 l/s , 30l/s and 20l/s , So that we get the accurate observation how the water profile made for high to low discharges.

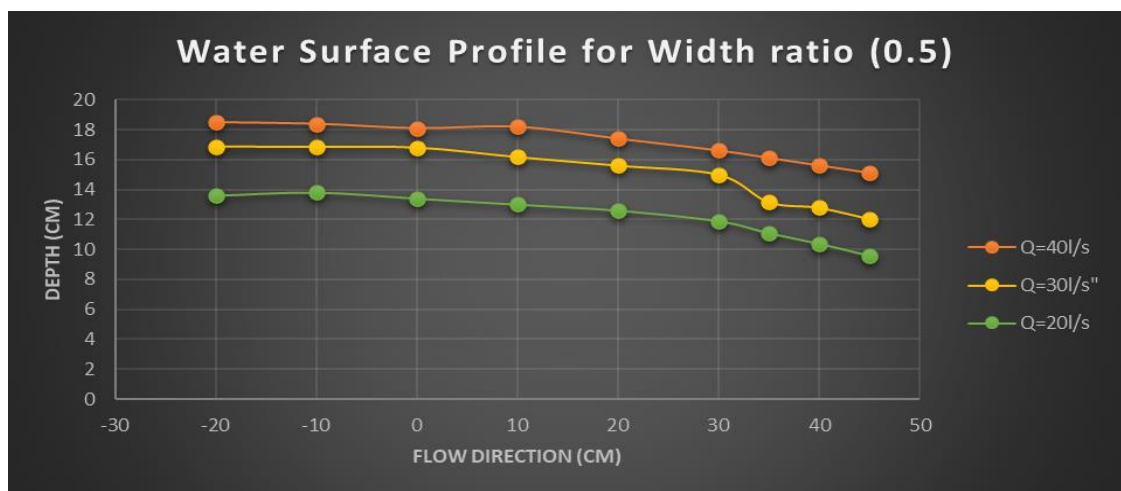


Figure 4.11. Water surface profile for width ratio (0.5)

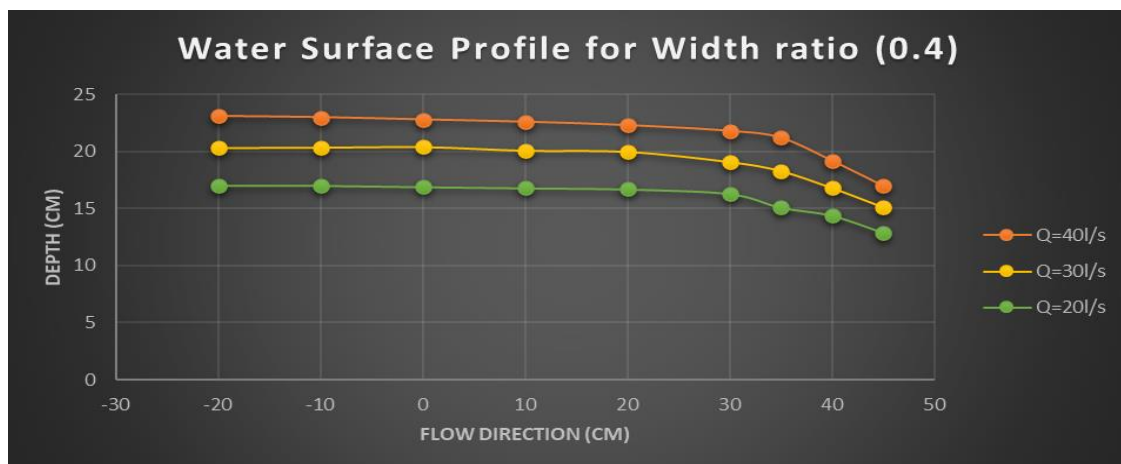


Figure 4.12 Water surface profile for width ratio (0.4)

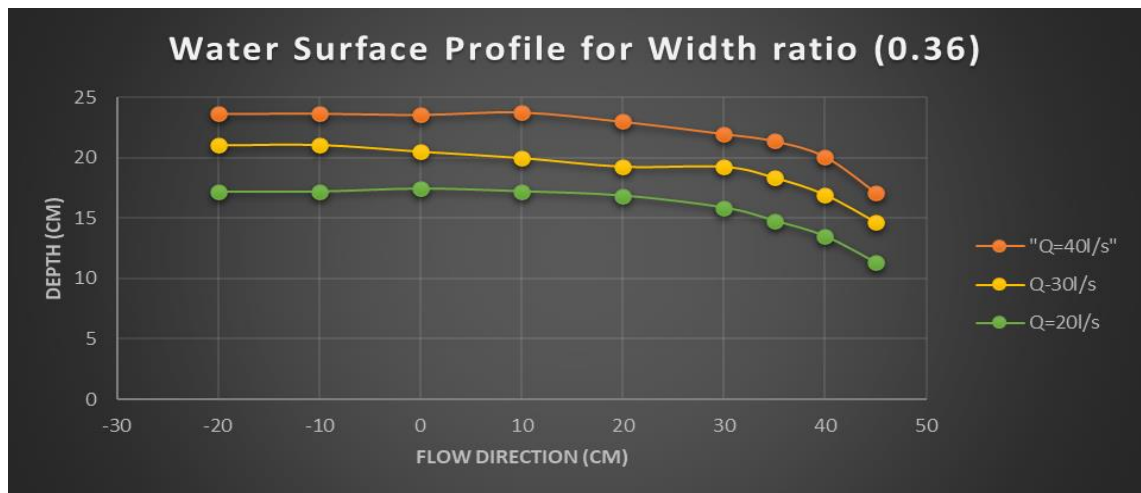


Fig 4.13 Water Surface profile for width ratio (0.36)

For the Figure number (4,11 to 4.13) , the water surface profile are plotted from the inlet to the throat of the venturiflume . These profiles are plotted with the three discharges changes from 40 l/s to 20 l/s , It is noted that the depth of the water increases with the increment of discharges as well as the width ratio.

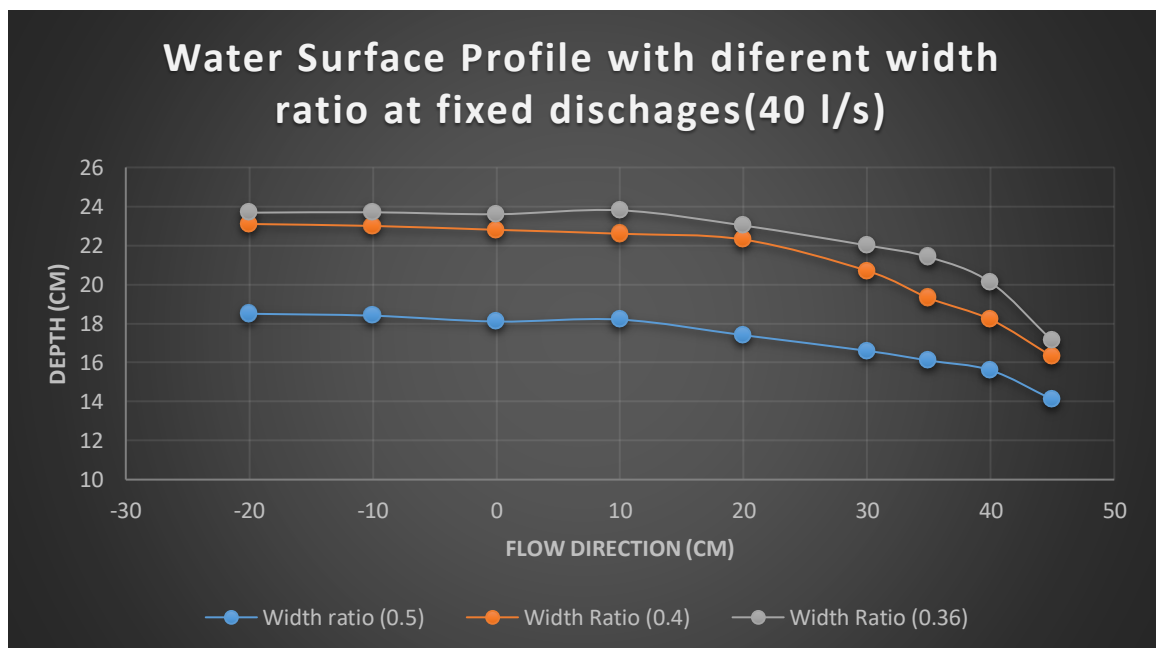


Figure 4.14 Water Surface Profile with different width ratio at fixed disc, (40 l/s)



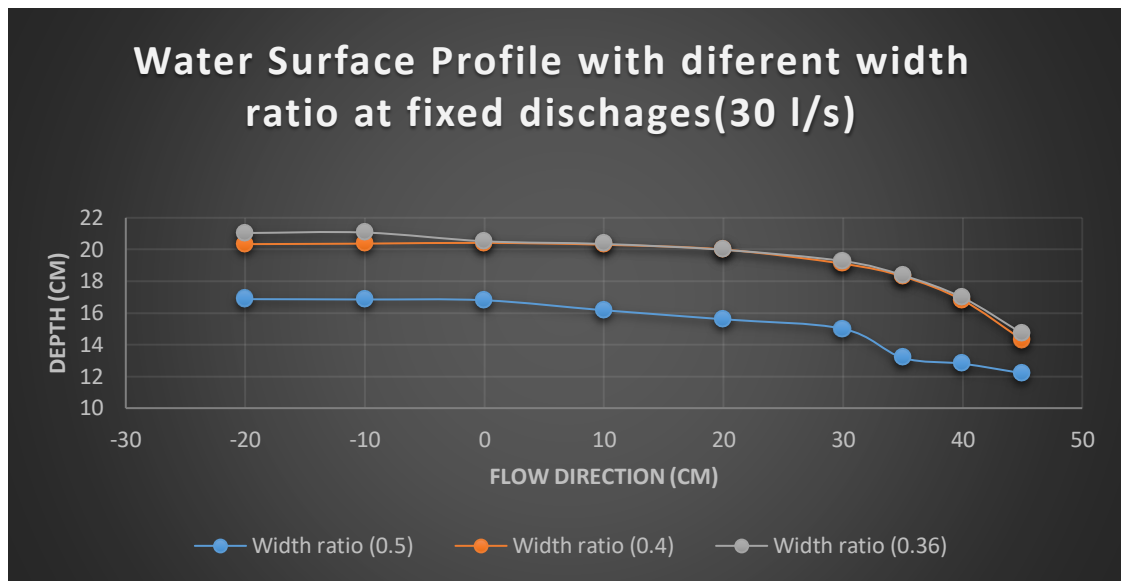


Figure 4.15 Water Surface Profile with different width ratio at fixed dis. (30 l/s)

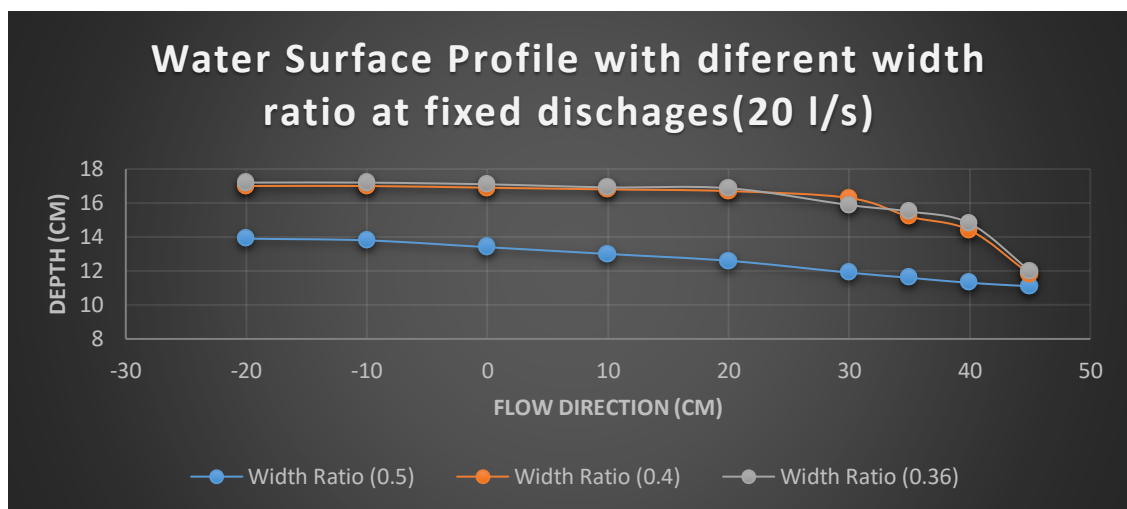


Figure 4.16 Water Surface Profile with different width fixed discharges (20 l/s)

In the Figure no 4.14 , the water profile are plotted finely and for the high discharges like (40l/s) ,the plot can be distinguished well ,It shows that as the width ratio decreases from 0.5 to 0.36 , the water surface profiles increases .But for the Figure no 4.15 , the medium discharge (30l/s) , the water profile nearly same for both the width 0.36 as well as the 0.4 .And also for the low discharges the water profile nearly go same for the these two width ratio , but for the 0.5 width ratio the water profile falls more than the above two width ratio.

## CHAPTER 5

### CONCLUSION

In this study various experiments were conducted on the flume vary different width ratio of venturi flume ranges from 0.5 to 0.36 with different discharges vary from 20l/s to 40 l/s at an increment of 5l/s.

From the results of the experiments , the following conclusions were arrived :

- I. For increased discharges , the depth at both the inlet and throat were found to increase for various width ratio.
- II. In the various width ratio it has been found for width ratio 0.36 the flow at the throat section is just critical and if we further decrease the flow may become critical.
- III. For high discharges ,water surface profile increses with the width ratio.But for the low the discharges the water surface for the 0.36 and 0.4 closesly move.
- IV. The Froude number is found to be increasing when the discharge is increasing. But it is interesting to see that the width ratio is decreasing but the Froude number at the throat section is going to critical.

Therefore it is concluded that for the venturiflume the width ratio of 0,36 is optimised.This is mainly useful while designing culvert whose minium waterway should be used for economic and efficient design of culverts .

## FUTURE SCOPE

The research may be extended with CFD studies and compare with the exponents for validation

The throat section can be studied for the future study

Various other types of flume can be compared and study of water profile can be done.

## REFERENCES

- [1]P. Sihag, O. F. Dursun, S. S. Sammen, A. Malik, and A. Chauhan, “Prediction of aeration efficiency of Parshall and Modified Venturi flumes: application of soft computing versus regression models,” *Water Supply*, vol. 21, no. 8, pp. 4068–4085, Jun. 2021, doi: 10.2166/ws.2021.161.
- [2]M. Heyrani, A. Mohammadian, I. Nistor, and O. F. Dursun, “Numerical Modeling of Venturi Flume,” *Hydrology*, vol. 8, no. 1, p. 27, Feb. 2021, doi: 10.3390/hydrology8010027.
- [3]B. Sun, L. Yang, S. Zhu, Q. Liu, C. Zhang, and J. Zhang, “Experimental and Numerical Investigation of Flow Measurement Mechanism and Hydraulic Performance of Portable Pillar-Shaped Flumes in Rectangular Channels,” *Shock and Vibration*, vol. 2020, pp. 1–17, Aug. 2020, doi: 10.1155/2020/8815957.
- [4]A. Zuikov and T. Suehtina, “Hydraulics of smoothly streamlined Venturi channels of critical depth,” *E3S Web of Conferences*, vol. 91, p. 07021, 2019, doi: 10.1051/e3sconf/20199107021.
- [5]A. L. Zuikov and V. V. Bakunyaeva, “Analytical Method of the Hydraulic Calculation of the Flow Rate of a Venturi Channel,” *Power Technology and Engineering*, vol. 51, no. 6, pp. 621–627, Mar. 2018, doi: 10.1007/s10749-018-0882-8.

[6]O. Castro-Orgaz, “Hydraulic design of Khafagi flumes,” *Journal of Hydraulic Research*, vol. 46, no. 5, pp. 691–698, Sep. 2008, doi: 10.3826/jhr.2008.3315.

[7]Y. Zerihun, “A Numerical Study on Curvilinear Free Surface Flows in Venturi Flumes,” *Fluids*, vol. 1, no. 3, p. 21, Jun. 2016, doi: 10.3390/fluids1030021.

[8]M. Dufresne and J. Vazquez, “Head–discharge relationship of Venturi flumes: from long to short throats,” *Journal of Hydraulic Research*, vol. 51, no. 4, pp. 465–468, Apr. 2013, doi: 10.1080/00221686.2013.781550.

[9 ] T.Gill & R. Finheling (2006) ,”Submerged Venturiflume”.

[10]M. EmiN. Emiroglu and A. Baylar, “Study of the influence of air holes along length of convergent-divergent passage of a venturi device on aeration,” *Journal of Hydraulic Research*, vol. 41, no. 5, pp. 513–520, Sep. 2003, doi: 10.1080/00221680309499996.

[11]S. J. Wright, B. P. Tullis, and T. M. Long, “Recalibration of Parshall Flumes at Low Discharges,” *Journal of Irrigation and Drainage Engineering*, vol. 120, no. 2, pp. 348–362, Mar. 1994, doi: 10.1061/(asce)0733-9437(1994)120:2(348).

[12]S. J. Wright and B. Taheri, “Correction to Parshall Flume Calibrations at Low Discharges,” *Journal of Irrigation and Drainage Engineering*, vol. 117, no. 5, pp. 800–804, Sep. 1991, doi: 10.1061/(asce)0733-9437(1991)117:5(800).

[13 ]B. Sun, L. Yang, S. Zhu, Q. Liu, C. Wang, and C. Zhang, “Study on the applicability of four flumes in small rectangular channels,” *Flow Measurement and Instrumentation*, vol.80,p.101967, Aug. 2021, doi: 10.1016/j.flowmeasinst.2021.101967.